

## Dislocation based stresses during electrochemical cycling and phase transformation in lithium-ion batteries

Pankaj Dhiman, Hsiao-Ying Shadow Huang\*

Mechanical and Aerospace Engineering Department, North Carolina State University, R3158 Engineering Building 3, Campus Box 7910, 911 Oval Drive, Raleigh, NC 27695, United States

### ARTICLE INFO

Dataset link: <https://huang.wordpress.ncsu.edu>

#### Keywords:

Lithium-ion battery  
Dislocations  
Stresses  
Cyclic voltammetry

### ABSTRACT

Lithium iron phosphate ( $\text{LiFePO}_4$ ) contains defects that play an important role in structural degradation of batteries. Linear defects called dislocations are introduced inside the lithium ion battery material during fabrication process accompanied by distortion produced stress fields around them. The present study deals with these mechanical stresses around dislocations in lithium iron phosphate and the change in stress field during phase transformation of lithium iron phosphate electrode material. A model consisting of multiple dislocations inside a lithium iron phosphate material incorporating anisotropic material properties is used to calculate stress fields using linear elastic theory and the superposition method. The stress fields around dislocations during phase transformation of lithium-iron phosphate are numerically calculated by incorporating the anisotropic properties of the material. The change in electrochemical behaviour of material due to change in stress field during phase transformation is also studied, where a modified electrochemical kinetics equation (i.e., Butler Volmer equation) is derived and used to account for dislocation induced stresses during the reversible cyclic voltammetry of the lithium iron phosphate. The results show the stress inside material does not remain constant during phase transformation and its variations are dislocation orientation dependent. In addition, the result shows that the presence of stress fields around dislocations changes the electrochemical behaviour of the material as suggested by the shift in the cyclic voltammograms. The effect of increasing scan rate on cyclic voltammogram is also studied for lithium iron phosphate. The results show that the increase in current at peaks is independent of the orientation of dislocations studied. Moreover, the decrease in current corresponding to a particular overvoltage value before anodic peak and increase in current after the anodic peak is found to be somehow proportional to the scan rate. Increased scan rates show increased deviation of current from a cyclic voltammogram for material in which there is no phase transformation. The results provide an insight into how presence of defects and phase transformation changes the electrochemical behaviour of the material. It is concluded that the combined effect of the stresses induced around dislocations during phase transformation and high scan rate can be used for modifying battery materials for various applications by changing electrochemistry of electrodes. The present study incorporates electrochemistry, defects and phase transformation into one battery chemistry and thus is important in our understanding of the Li-ion batteries.

### 1. Introduction

Lithium ion batteries having high gravimetric and volumetric energy density [1] have made possible the realization of electric vehicles (EVs), hybrid electric vehicles (HEVs) and plug in hybrid electric vehicles (PHEVs) reducing harmful environmental effects of internal combustion engines. Due to their high energy density, lithium ion batteries are also being used excessively in portable electronics including mobile phones and laptops. Lithium Cobalt Oxide ( $\text{LiCoO}_2$ ) is utilized in most portable electronics as the cathode material due to its

high energy density [2] but possesses safety risks [3] due to cobalt being toxic and  $\text{LiCoO}_2$  having low thermal stability [4]. Overcoming the limitations of  $\text{LiCoO}_2$ , an alternate cathode material was proposed by Goodenough in 1996 [5]. Despite having lower energy density than  $\text{LiCoO}_2$  does, lithium iron phosphate also known as LFP is a highly commercial used cathode material because of its longer life cycle, thermal stability, flat discharge voltage ( $\sim 3.6$  V vs  $\text{Li}^+/\text{LiO}$ ) and low price. Despite all these advantages, lithium iron phosphate suffers from low electrical conductivity [6]. However, electrical conductivity of lithium iron phosphate is shown to improve by doping of lithium iron

\* Corresponding author.

E-mail address: [hshuang@ncsu.edu](mailto:hshuang@ncsu.edu) (H.-Y.S. Huang).

phosphate with alien atoms, surface coatings or changing crystal morphology [7]. Characteristics of lithium iron phosphate such as high energy density and environmentally safe accompanied with long life cycle thus makes it a promising cathode material that has already been exploited in the batteries.

It has been suggested that cathode materials like lithium iron phosphate contains defects that may be formed during fabrication at a finite temperature due to a number of reasons. Previous research has shown how defects in lithium iron phosphate can be engineered to control material properties. Li et al. [8] evaluated the coupled effects of surface and dislocation mechanisms on diffusion induced stress in spherical nanoparticle electrode. They showed that the tensile stresses in spherical electrode are weakened by the coupled effect and even converted from tensile to compressive. Thus, the effect was considered useful suppressing cracks nucleation and propagation caused by the internal damage during battery charging and discharging cycles. Li et al. [9] analytically modelled the effect of dislocations on diffusion induced stresses in a cylindrical lithium ion battery electrode. They explained the combined effect of diffusion induced stresses and dislocations on preventing the crack nucleation and propagation under galvanostatic or potentiostatic conditions. Ulvestad et al. [10] studied the topological defect dynamics in operando battery nanoparticles using Bragg coherent diffractive imaging and reported the nucleation of lithium rich phase near the dislocations during the structural phase transformation. They also found out the material elastic properties to be considerably different from the bulk (i.e., negative Poisson's ratio) in the vicinity of dislocations at high voltage. The research supported the idea that dislocations can be used to tailor material properties.

The aim of this research is to study the dislocation-based stresses inside lithium iron phosphate during electrochemical cycling and phase transformation. The work is continuation of the work done by Huang and Wang [11] in which the effect of orientation of dislocations on stress field was studied in a lithium iron phosphate material. A model consisting of multiple dislocations inside a lithium iron phosphate material incorporating anisotropic material properties was used to calculate stress fields using linear elastic theory and superposition method. The stress fields around dislocations during phase transformation of lithium-iron phosphate were numerically calculated incorporating the anisotropic properties of the material. The change in scan-rate dependent electrochemical behaviour of material due to change in stress field during phase transformation transformation of lithium-iron phosphate was also studied, where a modified electrochemical kinetics equation (i.e., Butler Volmer equation) is derived and used to account for dislocation induced stresses during the reversible cyclic voltammetry of the lithium iron phosphate. The effect of increasing scan rate on cyclic voltammogram was also studied for lithium iron phosphate.

## 2. Methods

### 2.1. Stresses during phase transformation

The cathode material lithium iron phosphate in study has orthorhombic crystal structure and anisotropic elastic constants as given in Maxisch and Ceder (2006) [12]. LiFePO<sub>4</sub> exhibits a two-phase system with a single lithium poor phase called heterosite (FePO<sub>4</sub>) and lithium rich phase called triphylite (LiFePO<sub>4</sub>). Both phases are olivine type orthorhombic structures with the P<sub>nma</sub> space group although the lattice constants for both the phases differ and contribute to ~7% volumetric contraction from triphylite when heterosite is formed. The phase boundary between FePO<sub>4</sub> and LiFePO<sub>4</sub> is coherent which forms when two crystals match perfectly at the interface plane. An analytical solution of dislocation based stress field using anisotropic property was given by Indenbom and Lothe [13]. The solution held good for orthorhombic materials such as lithium iron phosphate where anisotropic properties cannot be ignored, and elastic constants varied in different

directions. The solution for stress fields of a dislocation with arbitrary Burgers vector was given by Eq. (2-1).

$$\begin{aligned} \sigma_{ij} &= \frac{b_x \lambda (C_{12} - \bar{C}_{11})}{4\pi q^2 t^2 \bar{C}_{11} C_{66} \sin \phi} \\ &\left\{ \begin{array}{l} C_{ij11} [(\bar{C}_{11} + C_{12} + C_{12})x^2y + \lambda^2 C_{66} y^3] - C_{ij12} \\ (\bar{C}_{11} + C_{12})(x^3 - \lambda^2 xy^2) \\ - \frac{C_{ij22}}{C_{22}} [(\bar{C}_{11} C_{12} + C_{12}^2 + 2C_{12} C_{66} + \bar{C}_{11} C_{66})x^2y - \bar{C}_{11} C_{66} \\ \lambda^2 y^3] \end{array} \right\} \\ &- \frac{b_y \lambda (C_{12} - \bar{C}_{11})}{4\pi q^2 t^2 \bar{C}_{11} C_{66} \sin \phi} \\ &\left\{ \begin{array}{l} C_{ij22} [(\bar{C}_{11} + C_{12} + C_{66})\lambda^2 xy^2 + C_{66} x^3] - C_{ij12} \\ (\bar{C}_{11} + C_{12})(\lambda^2 y^3 - x^2 y) \\ - \frac{C_{ij11}}{C_{11}} [(\bar{C}_{11} C_{12} + C_{12}^2 + 2C_{12} C_{66} + \bar{C}_{11} C_{66})\lambda^2 xy^2 - \bar{C}_{11} C_{66} \\ x^3] \end{array} \right\} \quad (2-1) \end{aligned}$$

where  $\bar{C}_{ij} = (C_{11} C_{22})^{1/2}$ ,  $\lambda = (C_{11}/C_{22})^{1/4}$ ,  $\phi = \frac{1}{2} \cos^{-1} \left( \frac{C_{12}^2 + 2C_{12} C_{66} - \bar{C}_{11}^2}{2\bar{C}_{11} C_{66}} \right)$ ,

$$q^2 = x^2 + 2xy\lambda \cos \phi + y^2 \lambda^2$$

and  $t^2 = x^2 - 2xy\lambda \cos \phi + y^2 \lambda^2$ .  $C_{ij}$  (i, j = 1, ..., 6) in Eq. (2-1) referred to the elastic constants of an orthorhombic material, x and y were the position coordinates at which the stress was to be calculated and  $b_x$  and  $b_y$  were the Burgers vectors.

The stresses around dislocations depend on the elasticity of the material being considered. The lithium-poor and lithium-rich phases formed during phase transformation of lithium iron phosphate have different material properties and thus have different elasticity. For our study, the change in elasticity of the material during phase transformation was taken into account by the amount of phase transformation that occurred in the material at any instant during electrochemical reaction. Elastic constants of the electrode material change as the lithium iron phosphate progressively under-went phase transformation. The change in elastic constant at any instant of phase transformation was given by Eq. (2-2).

$$[C_{ij}] = (1 - x_p)[C_{ij}]_{FePO_4} + x_p [C_{ij}]_{LiFePO_4}, \quad (2-2)$$

where  $x_p$  is the amount of phase transformation and varies from 0 to 1 during phase transformation.  $[C_{ij}]_{FePO_4}$  referred to the elastic constants of lithium poor phase,  $[C_{ij}]_{LiFePO_4}$  referred to the elastic constants of lithium rich phase, and  $[C_{ij}]$  referred to the elastic constants of the electrode material with  $x_p$  amount of phase transformation from lithium-poor phase to lithium-rich phase. The  $x_p$  equaled to 0 indicated that no phase transformation had taken place in material whereas  $x_p$  equaled to 1 indicated that all of the FePO<sub>4</sub> has changed to LiFePO<sub>4</sub> and corresponded to 100% phase transformation. The elastic constants for LiFePO<sub>4</sub> and FePO<sub>4</sub> were taken from Maxisch and Ceder (2006) [12].

The stresses at any instant of time during phase transformation were calculated by Eq. (2-1) by utilizing in the values of elastic constant obtained from Eq. (2-2) using the values provided from Maxisch and Ceder (2006) [12]. Since there existed multiple dislocations simultaneously in any material, we incorporated two dislocations in our model. Thus, the stresses inside lithium iron phosphate due to the occurrence of two simultaneous dislocations with arbitrary Burgers vector were calculated by the superposition principle. The stress at any point in material was equal to the sum of the stresses caused by an individual dislocation at that point considering the existence of that dislocation only in the material. Since multiple dislocations existed simultaneously in a material, we could incorporate many dislocations corresponding to a real-world material. But we chose 2 dislocations only to keep our model simple with less computational time. Also, two dislocations provided a better visual understanding of how the stress field changes

during the phase transformation as seen in the results shown later. The model dimensions of lithium iron phosphate with lattice constants of lithium iron phosphate taken from [14] were  $100L \times 60L$  with 60 unit cells of lithium iron phosphate where  $L = 10 \text{ \AA}$ . An actual lithium iron phosphate particle was reported to be several hundred nanometres [15] and thus could be represented conveniently by our model. Also the model size was big enough to avoid dislocation cores of  $4L \times 4L$  [16] where linear elastic theory fails. The model size of  $100L \times 60L$  also depicted the overall stress distribution without any boundary effects. Mathematica (Wolfram Research, Champaign, IL) [17] was used to numerically calculate the stresses given by Eq. (2-1) and obtain the stress values and distributions. The stress fields were numerically calculated for two dislocations during phase transformation of lithium iron phosphate. The two dislocations were fixed in their locations but differed in their orientation with respect to each other. The first dislocation was located at  $(x, y) = (20L, -12L)$  whereas the second dislocation was located at  $(x, y) = (40L, 24L)$  in the model. The orientation of one of the dislocation labelled dislocation 2 was fixed with Burger vector  $b_x = 1$  and  $b_y = 0$  while the orientation of the other dislocation labelled Dislocation 1 was varied by varying its Burgers vector.

## 2.2. Derivation of modified Butler-Volmer equation

The Butler-Volmer Equation provides the most fundamental relationship between current and applied potential but lacks the effect of mechanical stresses inside the electrode. For this propose the effect of hydrostatic stress caused by dislocations was incorporated in the Butler-Volmer equation. The modified Butler-Volmer equation similar to Lu et al. [18] given by Eq. (2-5) was then used to simulate cyclic voltammetry of lithium iron phosphate having dislocations. We started with chemical equilibrium states without mechanical stresses where the activation energies of cathodic and anodic reactions are identical, i.e.,  $\Delta G_{0c}^\ddagger = \Delta G_{0a}^\ddagger = \Delta G_0^\ddagger$ . The chemical equilibrium could be broken by the applied electric potential and mechanical stress. If the applied electric potential was changed by  $\Delta E = E - E^{0'}$ , then the free energy of the oxidized state would be lowered relative to the reduce state by  $F\Delta E$ . For every mole of lithium intercalation, the increase in elastic energy is equal to the work done by the mechanical stress, i.e.,  $\Delta W_e = -\sigma_h \Omega$  where  $\sigma_h$  is the hydrostatic stress inside the material,  $\Omega$  is the partial molar volume of lithium iron phosphate. Thus the change in free energy of the reduced state relative to the oxidized state is  $F\Delta E + \Delta W_e$ . This change in total free energy contributes to the change in activation energies of cathodic and anodic reactions according to the charge transfer coefficients  $\alpha$  and  $(1-\alpha)$ :

$$\begin{aligned} \Delta G_c^\ddagger &= \Delta G_0^\ddagger + \alpha F\Delta E + \alpha \Delta W_e \\ \Delta G_a^\ddagger &= \Delta G_0^\ddagger - (1-\alpha)F\Delta E - (1-\alpha)\Delta W_e \end{aligned} \quad (2-3)$$

Assuming the rate constants have an Arrhenius form [19]:

$$\begin{aligned} k_f &= A_f \exp(-\Delta G_c^\ddagger/RT) \\ k_b &= A_b \exp(-\Delta G_a^\ddagger/RT) \end{aligned} \quad (2-4)$$

and proceeding in a regular manner as in deriving Butler-Volmer equation, the modified Butler Volmer equation was obtained:

$$\begin{aligned} i &= i_0 \left( \frac{C_O(0, t)}{C_O^*} \exp \left[ -\alpha \frac{F(E - E^{0'}) - \sigma_h \Omega}{RT} \right] - \frac{C_R(0, t)}{C_R^*} \right. \\ &\quad \left. \exp \left[ (1-\alpha) \frac{F(E - E^{0'}) - \sigma_h \Omega}{RT} \right] \right) \end{aligned} \quad (2-5)$$

Here  $R$  is the universal gas constant,  $T$  is the temperature,  $\alpha$  is the charge transfer coefficient,  $C_O^*$  and  $C_R^*$  are the bulk concentration of oxidized and reduced species,  $E - E^{0'}$  is the applied overpotential,  $\sigma_h$  is the hydrostatic stress inside the material,  $\Omega$  is the partial molar volume

of lithium iron phosphate and  $i_0$  is the exchange current density.

## 2.3. Phase transformation during electrochemical cycling

The over potential and phase transformation in storage electrodes was related by Tang et al. [20] with applications to nanoscale olivines. The paper served as a base for the research in studying the effect of mechanical stress in cyclic voltammetry (CV). During CV, the applied over-potential changed the phase of the lithium iron phosphate which varied the hydrostatic stress around edge or screw dislocations in the particle. This change in hydrostatic stress changed the current as per the modified Butler-Volmer equation. A phase transition from crystalline  $\text{LiFePO}_4$  to crystalline  $\text{FePO}_4$  is thermodynamically favourable at  $\Delta\phi$  (overpotential)  $> 0$ . However, such transitions need to overcome energy barriers (or activation energies) and the probability of the thermally activated transition is proportional to  $\exp(-\Delta F/kT)$ . Tang et al. [20] calculated the variation of activation energy  $\Delta F$  with increasing overpotential for transformation of a particle of  $r = 1 \mu\text{m}$  of crystalline  $\text{LiFePO}_4$  to crystalline  $\text{FePO}_4$ . The activation energy decreased with increased overpotential and evolved toward zero at a critical overpotential  $\Delta\phi_c = 30.283 \text{ mV}$ . Above this overpotential, the phase transformation was barrier less and occurred spontaneously. The activation energy,  $\Delta F$  decreased almost linearly with increased overpotential up to the point where it became zero. Due to thermally activated transition being proportional to  $\exp(-\Delta F/kT)$ , the phase transformation of crystalline  $\text{LiFePO}_4$  to crystalline  $\text{FePO}_4$  was considered to be exponential. Thus, a sigmoid function was used in our model to show the variation of phase transformation from 0 to  $\Delta\phi_c = 30.283 \text{ mV}$ .

A relation between mechanical stresses and phase transformation was developed first followed by a relation between applied overvoltage and phase transformation. The effect of changing stress field around dislocations during phase transformation was then studied by combining the knowledge of the two. The hydrostatic stress around dislocation was then calculated using Eq. (2-6) at any instance of cyclic voltammetry corresponding to an amount of phase transformation happened at that instant.

$$\sigma_h = \frac{\sigma_{xx} + \sigma_{yy} + \sigma_{zz}}{3} \quad (2-6)$$

Based on Eq. (2-1), the stress field could be obtained. The inverse of cosine would result in complex variables by using the orthotropic elastic constant. In this study, the imaginary component of the hydrostatic stress was negligible to avoid numerical issues while simulating cyclic voltammograms. The hydrostatic stress thus calculated at any instance of cyclic voltammetry corresponding to a particular amount of phase transformation was then used in the modified Butler Volmer equation (Eq. (2-5)) to simulate the cyclic voltammogram.

## 3. Results and discussion

Fig. 1 showed the results of the stress evaluation of stress field during phase transformation with dislocation 1 having Burgers vector  $b_x = 1$ ,  $b_y = 0$  and dislocation 2 with Burgers vector  $b_x = 1$ ,  $b_y = 0$  (configuration 1). Thus, both the dislocations had the same orientations by having the same Burgers vectors in this case. The amount of phase transformations tabulated against stresses in Fig. 1 were chosen to correspond with  $x_p = 0.2$ ,  $x_p = 0.6$  and  $x_p = 0.9$ . These values were chosen because they showed the maximum difference in stress fields during phase transformation and represent the phenomenon visually. As shown in the Fig. 1, the stresses increased with increased amount of phase transformation. Thus, as the phase transformation from  $\text{FePO}_4$  to  $\text{LiFePO}_4$  inside the cathode material started proceeding, the material also started experiencing more dislocation-based stresses. The increase in the stresses was proportional to the density of dislocations inside the material. It was also seen from Fig. 1 that  $\sigma_{xx}$  showed the most variation during the phase transformation whereas  $\sigma_{yy}$  showed the least

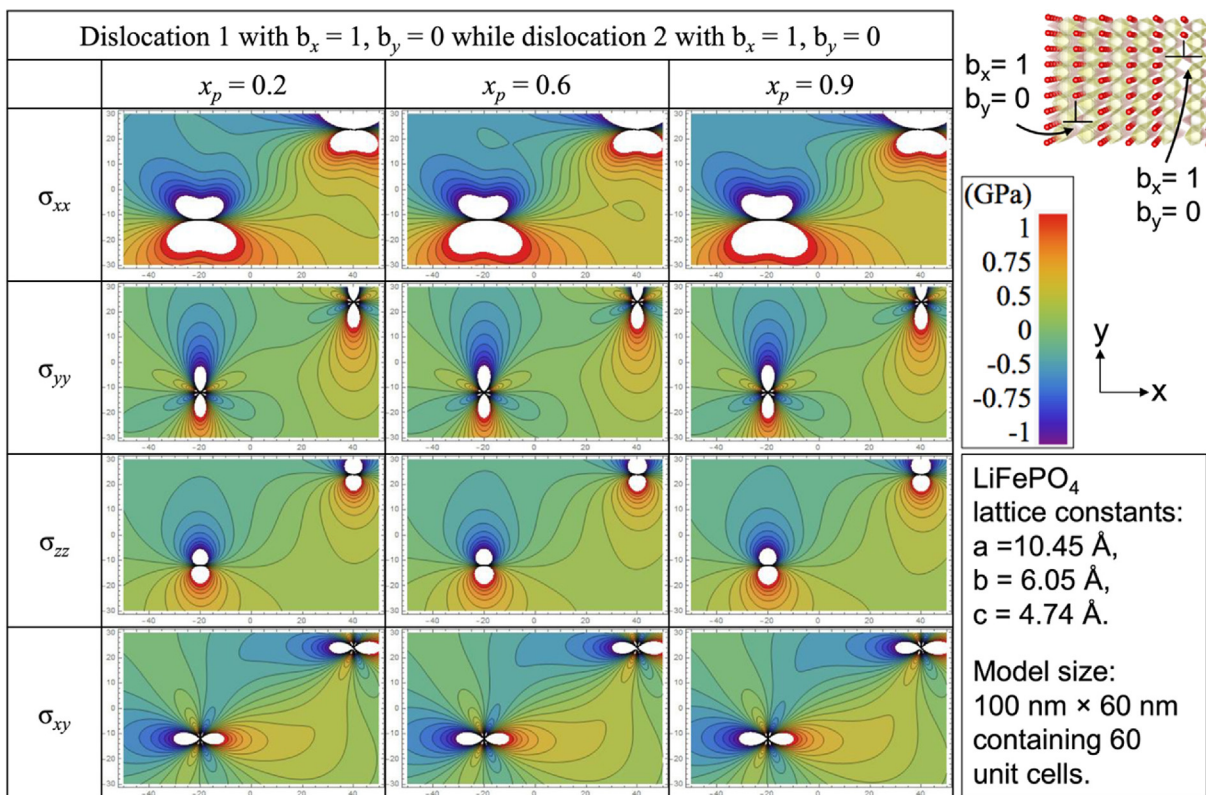


Fig. 1. Stress field of 1st type dislocation configuration during phase transformation, where dislocation 1 with Burgers vectors  $b_x = 1, b_y = 0$  and dislocation 2 with Burgers vector  $b_x = 1, b_y = 0$ .  $x_p$  was the amount of phase transformation and varies from 0 to 1 during phase transformation.

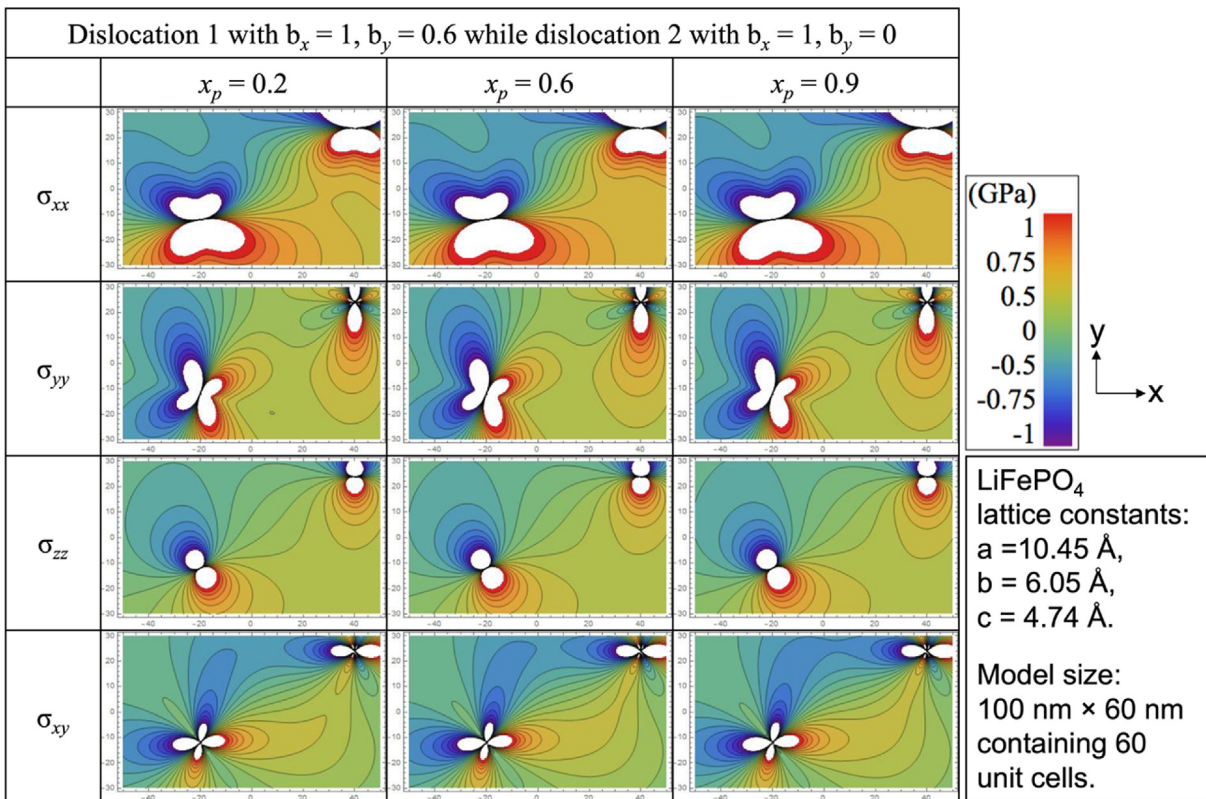
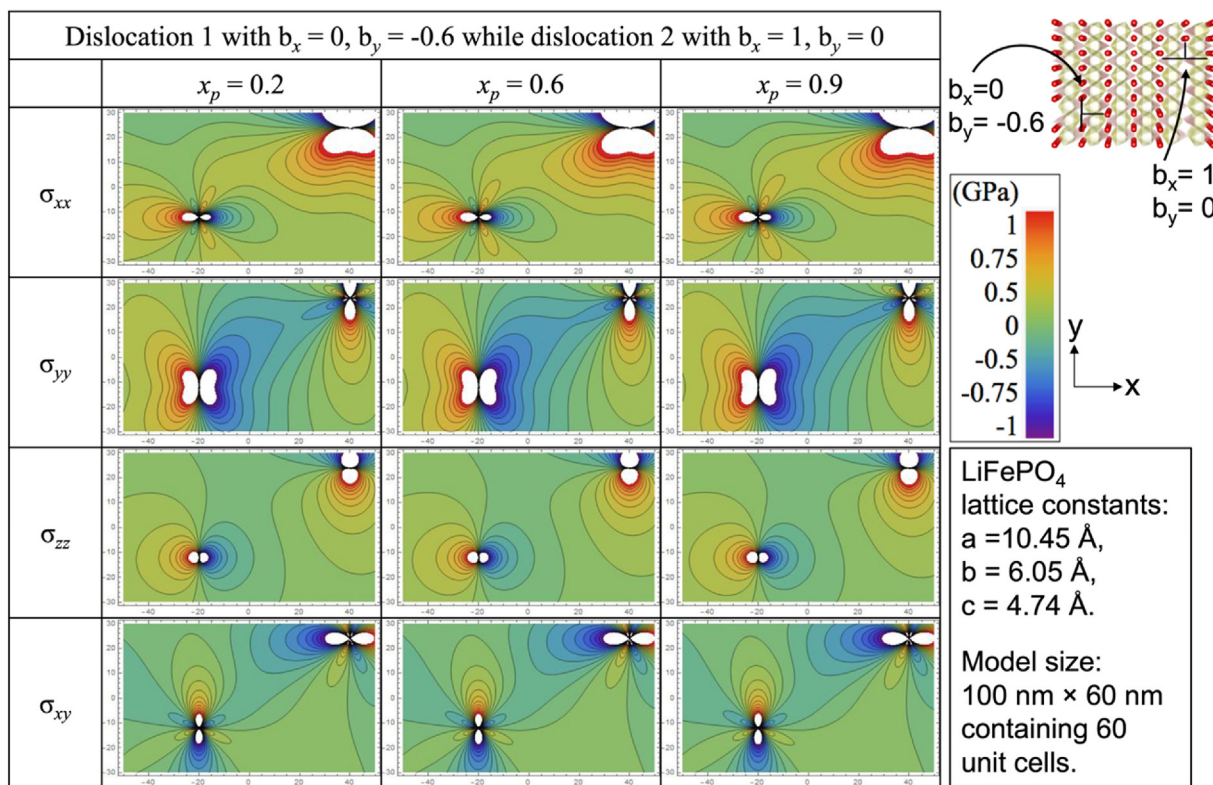


Fig. 2. Stress field of 2nd type dislocation configuration during phase transformation, where dislocation 1 with Burgers vectors  $b_x = 1, b_y = 0.6$  and dislocation 2 with Burgers vector  $b_x = 1, b_y = 0$ .  $x_p$  was the amount of phase transformation and varies from 0 to 1 during phase transformation.



**Fig. 3.** Stress field of 3rd type dislocation configuration during phase transformation, where dislocation 1 with Burgers vectors  $b_x = 0$ ,  $b_y = -0.6$  and dislocation 2 with Burgers vector  $b_x = 1$ ,  $b_y = 0$ .  $x_p$  was the amount of phase transformation and varies from 0 to 1 during phase transformation.

variation. Fig. 2 showed the results of the stress evaluation of different stresses during phase transformation with dislocation 1 having Burgers vector  $b_x = 1$ ,  $b_y = 0.6$  and dislocation 2 with Burger vector  $b_x = 1$ ,  $b_y = 0$  (configuration 2). Thus, both the dislocations do not had the same orientation anymore in this case. The dislocation 2 was fixed in this orientation while the orientation of dislocation 1 was changed. As shown in the Fig. 2, the stresses in this case also increased with increased amount of phase transformation. It was also seen from Fig. 2 that all the stresses increased considerably during phase transformation as more and more  $\text{FePO}_4$  changed to  $\text{LiFePO}_4$  compared to Fig. 1 where  $\sigma_{xx}$  showed the most variation during the phase transformation and  $\sigma_{yy}$  showed the least variation and almost did not change. Fig. 3 showed the results of the stress evaluation of different stresses during phase transformation with dislocation 1 having Burgers vector  $b_x = 0$ ,  $b_y = -0.6$  and dislocation 2 with Burger vector  $b_x = 1$ ,  $b_y = 0$  (configuration 3). Compared to Figs. 1 and 2, the stresses during phase transformation in Fig. 3 did not increase as  $\text{FePO}_4$  was progressively changed to  $\text{LiFePO}_4$ . On the contrary, they decreased because of the particular orientation in which the two dislocations were oriented. Thus, it can be argued the increase or decrease in stresses around dislocations depends on the orientation of dislocations. Also comparing Figs. 1 and 2, it was observed that the change in stress in a particular direction was also dependent on orientation of dislocation. Fig. 1 showed that  $\sigma_{xx}$ ,  $\sigma_{zz}$  and  $\sigma_{xy}$  changed significantly during the phase transformation whereas  $\sigma_{yy}$  almost did not change. However, the orientation of two dislocations in Fig. 2 corresponded to significant changes in all components of stresses.

The CV curves obtained using the modified Butler-Volmer equation (Eq. (2-5)) with partial molar volume of lithium iron phosphate taken to be in the order of  $10^{-4}$  were shown in Fig. 4 for three different orientations of two dislocations. The partial molar volume of lithium iron phosphate was taken to be in the order of  $10^{-4}$  to account for the mechanical stresses associated with the introduction of dislocations in the material. It was seen that partial molar volume of the order of  $10^{-5}$  or lower had no significant shift in the shape of the CV curve with the

introduction of dislocations in the material. Therefore, any value larger than  $10^{-4}$  would further alter the CV curves, i.e., electrochemical behaviors of the electrodes. The region of phase transformation was shown in grey color inside the CV curve and it was seen that the stress changes inside the material during phase transformation due to which the CV curves for phase transformation and without phase transformation were different. A typical CV curve for an electrochemically reversible reaction without any stresses was also shown alongside with blue dotted lines for comparison. It can be concluded that the dislocations can be useful for changing the characteristics of CV curve and thus can be used for designing batteries for various applications by changing the electrochemistry of electrode battery accordingly. For example, it was observed that the current decreased for the same overpotential due to the stresses induced by dislocations for certain overpotential range (between anodic peak and zero overpotential for forward scan). The reverse effect of increasing current for the same overvoltage can be created if the nature of stress (compressive or tensile) was changed by varying orientation of dislocations. Thus, low current or high current can be obtained for the same voltage in a CV curve depending on difference usages. Comparing Fig. 4(a)–(c), it was observed that the reduction in current due to phase transformation in anodic scan (before anodic peak) for the same overpotential was more obvious in Fig. 4(b) than one shown in Fig. 4(a). This was attributed to the particular orientation of the dislocations corresponding to the cyclic voltammograms considered. In addition, comparing Fig. 4(b) and (c), this reduction in current was almost the same for a particular overpotential because both CV curves corresponded to the dislocations oriented in such a way that they produced almost equal average hydrostatic stress inside the material. Thus, three important observations were made from Fig. 4:

1. The presence of dislocations changed the electrochemical performance of electrodes dramatically which were revealed by the shift of the shape of the CV curve, as shown by comparing the blue dotted

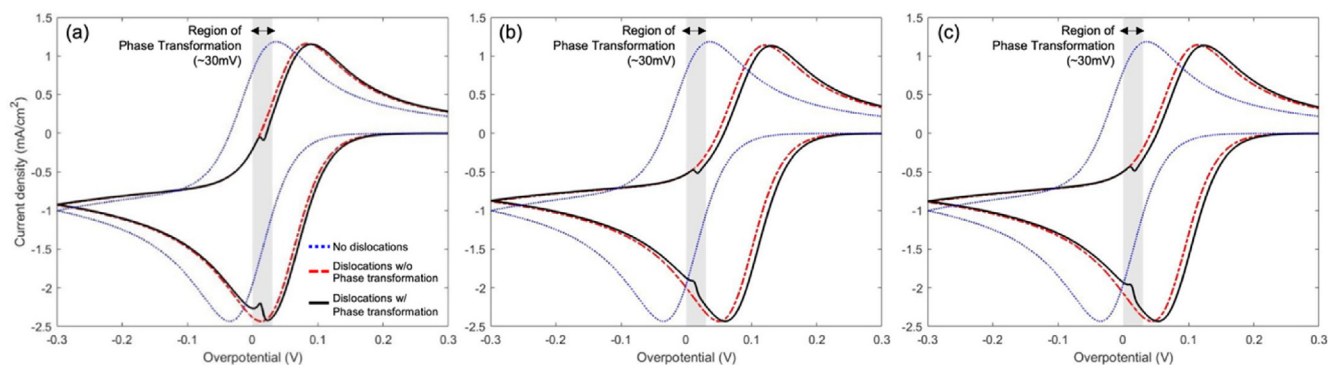


**Fig. 4.** CV curve for 3 different orientations of two dislocations with in lithium iron phosphate material. (a) Dislocation 1 with Burgers vectors  $b_x = 1$ ,  $b_y = 0$  and dislocation 2 with Burgers vector  $b_x = 1$ ,  $b_y = 0$ . (b) Dislocation 1 with Burgers vectors  $b_x = 1$ ,  $b_y = 0.6$  and dislocation 2 with Burgers vector  $b_x = 1$ ,  $b_y = 0$ . (c) Dislocation 1 with Burgers vectors  $b_x = 0$ ,  $b_y = -0.6$  and dislocation 2 with Burgers vector  $b_x = 1$ ,  $b_y = 0$ .

curves (without stress) and red dashed curves (with stress) in Fig. 4. This change in shape is attributed to the presence of stresses around dislocations.

2. Phase transformation inside lithium iron phosphate electrode having dislocations caused further change in electrochemical performance of the electrode as seen by comparing red dashed curves (without phase transformation) and black solid curves (with phase transformation) in Fig. 4. As soon as the phase transformation started inside the material due to applied overvoltage, the stress field around dislocations changed along with its electrochemical behavior. The more the phase transformation occurred by increasing overpotential, the current reduced more with respect to its value without having any phase transformation up to the anodic peak and then increased beyond the anodic peak. The reverse phenomenon happened for the cathodic peak.
3. The cyclic voltammograms with dislocation oriented as shown in Fig. 4(b) and (c) had almost identical CV curves because both CV curves corresponded to the dislocations oriented in such a way that they produced almost equal average hydrostatic stress inside the material. Thus, it can be concluded that different orientation of dislocations can be used to change the electrochemical behavior of the electrode in the same way. This is due to the nearly same hydrostatic stress produced by the two orientation of dislocations irrespective of having different stress fields for the individual components of stress.

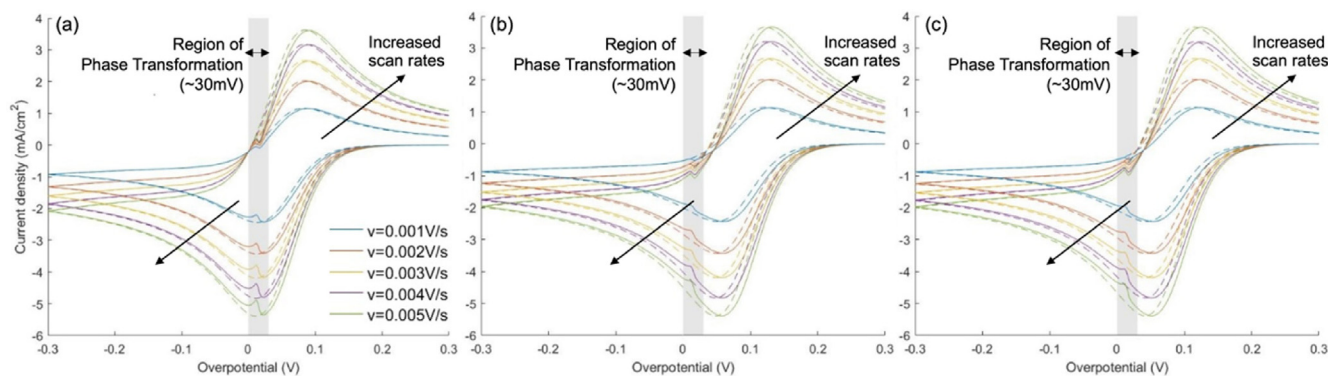
Thus, it can be concluded from Fig. 4 that presence and orientation of two dislocations during phase transformation were the two primary factors that affect the electrochemical behaviour of the material during battery charge-discharge cycles.

Fig. 5 showed the effect of increasing the scan rate of the forward and backward scan on the CV curve. It was seen that increasing the scan rate increased the current for the applied over-voltage for all the three different orientations of the dislocations studied. The dashed lines in Fig. 5 showed the CV curves without phase transformation and solid lines showed CV curves with phase transformation corresponding to a particular scan rate. The key observations from Fig. 5 were as follows:

1. The increase in current for a particular overvoltage was a phenomenon that was independent of the orientation of dislocations considered in our model.
2. The decrease in current corresponding to a particular overvoltage value before anodic peak and increase in current after the anodic peak was somehow proportional to the scan rate.
3. Increased scan rates showed increased deviation of current from a CV curve for material in which there was no phase transformation.

The observed increase in the current for increased scan rate can be explained in terms of diffusion layer size. The diffusion layer grew much farther from the electrode with a low voltage scan rate than in a high voltage scan rate. Thus, the flux to the electrode surface was considerably smaller at slow scan rates compared to one with the faster scan rates and hence the current was also smaller at slow scan rates. It was also seen that the linear increase or decrease in scan rate did not cause linear variation in the current for the same overpotential. This was due to the inherent nature of the Butler-Volmer equation in which the overpotential terms was raised exponentially and any change in overpotential at any scan rate consequently did not cause linear variation in current.

It is known that when two or more dislocations are close to each



**Fig. 5.** Effect of scan rate on CV curve for three different orientations of two dislocations in lithium iron phosphate electrode material. (a) Dislocation 1 with Burgers vectors  $b_x = 1$ ,  $b_y = 0$  and dislocation 2 with Burgers vector  $b_x = 1$ ,  $b_y = 0$ . (b) Dislocation 1 with Burgers vectors  $b_x = 1$ ,  $b_y = 0.6$  and dislocation 2 with Burgers vector  $b_x = 1$ ,  $b_y = 0$ . (c) Dislocation 1 with Burgers vectors  $b_x = 0$ ,  $b_y = -0.6$  and dislocation 2 with Burgers vector  $b_x = 1$ ,  $b_y = 0$ .

other, forces of attraction or repulsion occur to reduce the total elastic energy. We have published the calculations of the force field resulted from interactions of dislocations [11], where forces  $[F] = [\sigma][b] \times [n]$ ; the force vector was determined by the stress field  $[\sigma]$  of dislocation 1 and Burgers vectors  $[b]$  of dislocation 2, and  $[n]$  was the normal direction of the plane. We have observed that for two parallel edge dislocations, the closer they were, the stronger the attractive or repulsive forces were between them, suggesting the dislocations tended to reduce the total elastic energy by repelling each other. As for two parallel edge dislocations with the same Burgers vectors or opposite Burgers vectors, similar but opposite effects occurred, and it was suggested that two dislocations with opposite signs tended to meet each other and cancelled out the forces between them. Moreover, we could speculate that dislocations could move relatively due to forces of attraction or repulsion. In this case, the distance between two dislocations would consequently change, and the stress fields between them could be easily recalculated by reassigning the position coordinates (i.e.,  $x$  and  $y$ ) in Eq. (2-1).

#### 4. Conclusion

The research dealt with studying the effect of dislocation-based stresses during phase transformation of a lithium iron phosphate cathode on a cyclic voltammogram. A model consisting of two dislocations inside a lithium iron phosphate material was used to calculate stress fields using linear elastic theory and the superposition method. The stress fields around dislocations during phase transformation of  $\text{LiFePO}_4$  were then numerically simulated incorporating the anisotropic properties of the material. The results showed that the stress inside material increase or decrease during phase transformation and did not remain constant. The variations in stress depended on the orientation of the dislocations. While in one case, some dislocations were oriented in such a way that they increased the overall stress as opposed to the other case in which they were oriented to decrease the overall stress. Also, it was observed that the amount of increase of a particular component of stress during phase transformation was dependent on orientation of dislocations. While one orientation showed significant increase in all components of stress, the other orientation corresponded to significant increase only in some of the components with some remaining nearly constant throughout the phase transformation. A modified Butler-Volmer equation was used in simulating the reversible cyclic voltammogram of the lithium iron phosphate. The effect of stress caused by dislocations during phase transformation was also incorporated. It was observed that the presence of dislocations changed the electrochemical behaviour of the electrode material by shifting the CV curves. This change in electrochemical behaviour was attributed to the presence of stresses around dislocations. The current reduced significantly with respect to its value without having any phase transformation up to the anodic peak and then increased beyond the anodic peak. The reverse phenomenon also happened for the cathodic peak. It was also concluded that different orientations of dislocations can be used to change the electrochemical behavior of the electrode in same way. This was due to the nearly same hydrostatic stress produced by the two orientation of dislocations irrespective of having different stress fields for the individual components of stress. The effect of increasing scan rate was also studied on cyclic voltammogram for lithium iron phosphate. The increase in current at peaks was found independent of the orientation of dislocations considered. Also, the decrease in current corresponding to a particular overvoltage value before an anodic peak and increase in current after the anodic peak was found to be somehow proportional to the scan rate. Increased scan rates showed increased deviation of current from a CV curve for material in which there was no phase transformation. The results provided an insight into how presence of defects and phase transformation changes the electrochemical behaviour of the material. It was concluded that the combined effect of the stresses induced around dislocations and their orientation during

phase transformation can be used for creating batteries with electrodes having desired electrochemical behavior at particular overvoltage. Thus, defects inside battery electrodes can be engineered to change the electrochemical behaviour of the material, an example of which was the orientation and dislocation density considered in this work. Further study extending this work should include developing and using a similar model to understand the effect of dislocation-based stresses during phase transformation on electrochemical behaviour of another battery material chemistry, e.g., lithium nickel manganese cobalt oxide (NMC). Also, more than two dislocations can be considered in future work corresponding to high dislocation density in the material.

#### CRediT authorship contribution statement

**Pankaj Dhiman:** Conceptualization, Data curation, Formal analysis, Investigation, Methodology, Validation, Visualization, Writing - original draft. **Hsiao-Ying Shadow Huang:** Conceptualization, Investigation, Methodology, Project administration, Resources, Software, Supervision, Validation, Writing - review & editing.

#### Conflict of interest

The authors declare no conflict of interest.

#### Data availability

The raw data required to reproduce these findings are available to download from <https://huang.wordpress.ncsu.edu>. The processed data required to reproduce these findings are available to download from <https://huang.wordpress.ncsu.edu>.

#### References

- [1] X.P. Gao, H.X. Yang, Multi-electron reaction materials for high energy density batteries, *Energy Environ. Sci.* (2010).
- [2] Y. Takahashi, S. Tode, A. Kinoshita, H. Fujimoto, I. Nakane, S. Fujitani, Development of lithium-ion batteries with a  $\text{LiCoO}_2$  cathode toward high capacity by elevating charging potential, *J. Electrochem. Soc.* 155 (7) (2008) A537.
- [3] A. Mauger, C.M. Julien, Critical review on lithium-ion batteries: are they safe? sustainable? *Ionics (Kiel)* 23 (8) (Aug. 2017) 1933–1947.
- [4] K.-H. Choi, J.-H. Jeon, H.-K. Park, S.-M. Lee, Electrochemical performance and thermal stability of  $\text{LiCoO}_2$  cathodes surface-modified with a sputtered thin film of lithium phosphorus oxynitride, *J. Power Sources* 195 (24) (Dec. 2010) 8317–8321.
- [5] A.K. Padhi, Phospho-olivines as positive-electrode materials for rechargeable lithium batteries, *J. Electrochem. Soc.* (1997).
- [6] A. Awarke, S. Lauer, S. Pischinger, M. Wuttler, Percolation-tunneling modeling for the study of the electric conductivity in  $\text{LiFePO}_4$ -based Li-ion battery cathodes, *J. Power Sources* (2011).
- [7] P. Wang, et al., Improved electrochemical performance of  $\text{LiFePO}_4$ @N-doped carbon nanocomposites using polybenzoxazine as nitrogen and carbon sources, *ACS Appl. Mater. Interfaces* (2016).
- [8] J. Li, D. Lu, Q. Fang, Y. Liu, P. Wen, Cooperative surface effect and dislocation effect in lithium ion battery electrode, *Solid State Ionics* 274 (2015) 46–54.
- [9] J. Li, Q. Fang, F. Liu, Y. Liu, Analytical modeling of dislocation effect on diffusion induced stress in a cylindrical lithium ion battery electrode, *J. Power Sources* 272 (2014) 121–127.
- [10] A. Ulvestad et al., Topological defect dynamics in operando battery nanoparticles.
- [11] H.-Y. Shadow Huang, Y.-X. Wang, Dislocation based stress developments in lithium-ion batteries, *J. Electrochem. Soc.* 159 (6) (2012) A815.
- [12] T. Maxisch, G. Ceder, Elastic properties of olivine  $\text{Li}_x\text{FePO}_4$  from first principles, *Phys. Rev. B* 73 (17) (2006) 1–4.
- [13] V.L. Indenbom, J. Lothe, *Elastic Strain Fields and Dislocation Mobility*, North-Holland, 1992.
- [14] A. Andersson, B. Kalska, Lithium extraction/insertion in  $\text{LiFePO}_4$ : an X-ray diffraction and Mossbauer spectroscopy study, *Solid State Ionics* (2000).
- [15] N. Meethong, H.-Y.S. Huang, W.C. Carter, Y.-M. Chiang, Size-dependent lithium miscibility gap in nanoscale  $\text{Li}_{1-x}\text{FePO}_4$ , *Electrochem. Solid-State Lett.* 10 (5) (2007) A134.
- [16] R.P.V. Richard, W. Hertzberg, Jason L. Hertzberg, *Deformation and Fracture Mechanics of Engineering Materials*, John Wiley & Sons, Inc., ©2013, Hoboken, NJ, 2013.
- [17] I. Wolfram Research, *Mathematica*, Wolfram Research, Inc., Champaign, Illinois, 2018.
- [18] B. Lu, Y. Song, Q. Zhang, J. Pan, Y.T. Cheng, J. Zhang, Voltage hysteresis of lithium ion batteries caused by mechanical stress, *Phys. Chem. Chem. Phys.* 18 (6) (2016)

- 4721–4727.
- [19] L.R.F. Allen, J. Bard, *Electrochemical Methods : Fundamentals and Applications*, Wiley, New York, 2001.
- [20] M. Tang, N. Meethong, W.C. Carter, Model for the particle size, overpotential, and strain dependence of phase transition pathways in storage, in: M. EleTang, N. Meethong, W.C. Carter (Eds.), *Model for the Particle Size, Overpotential, and Strain Dependence of Phase Transition Pathways*, 2009, pp. 1557–1571.